



Structural Arrangements of Polymers Adsorbed at Nanostrings

Thomas Vogel*, Michael Bachmann¹

*Soft Matter Systems Research Group, Institut für Festkörperforschung (IFF-2),
Forschungszentrum Jülich, 52428 Jülich, Germany*

Abstract

We study ground states of a hybrid system consisting of a polymer and an attractive nanowire by means of computer simulations. Depending on structural and energetic properties of the substrate, we find different adsorbed polymer conformations, amongst which are spherical droplets attached to the wire and monolayer tubes surrounding it. We construct the complete conformational phase diagram and analyze in more detail particularly interesting polymer-tube conformations. © 2010 Published by Elsevier B.V.

Keywords: polymer, adsorption, nanotube, nanocylinder, droplet

1. Introduction

The study of the interaction between organic and inorganic matter, or in other words, the behavior of organic–inorganic systems, generates fascinating findings with potential for novel applications in bio- and nanotechnology. One of the basic steps in the understanding of such systems is the study of the adsorption of soft materials like polymers at inorganic matter like solid substrates. In the past, numerous computational studies gave general insights in the adsorption behavior of polymers on planar surfaces [1–5]. A particularly surprising fact for example, predicted by computer simulations and verified by experiments recently, is that a single specific mutation in a short peptide can substantially change the binding behavior to semiconductor substrates [6, 7].

A special class of such hybrid systems are nanotubes or nanocylinders interacting with polymers. Carbon nanotubes, for example, are themselves quite interesting nanostructures with surprising electronic and mechanical properties [8], but nanotube–polymer composites promise to enlarge the number of possible novel applications dramatically, for example in photonics and molecular sensor technologies [9, 10]. Theoretically, experimentally and computationally well studied is the wetting of cylindrical substrates by liquids or polymer droplets. This transition

*Corresponding author. E-mail: t.vogel@fz-juelich.de

¹E-mail: bachmann@smsyslab.org, Web: <http://www.smsyslab.org>

can be described by the crossover of barrel-like and clamshell-like droplets [11–13]. In another study, the adsorption behavior of individual polymer chains on nanotubes has been studied, where a helical-like winding of flexible and semi-flexible chains around the tubes was found [14].

In contrast, we will here develop a general picture of the adsorption behavior of polymers at nanowires depending on the properties of the substrate [15]. For this purpose, we apply a model, where the effective thickness and the attraction strength of the linelike substrate are variable parameters. The above mentioned transitions and adsorbed polymer structures are included as special cases in this picture.

2. Model and method

In our study the polymer is represented by a coarse-grained off-lattice bead–stick model, i.e., monomers do not have any inner structure and are connected by stiff bonds. The polymer is embedded into a three-dimensional simulation box which includes an attractive thin string pointing into the z -direction. The chain is not grafted to the string and may move freely. The monomers interact with each other via a standard Lennard-Jones potential

$$V_{\text{LJ}}(r_{ij}; \epsilon_m, \sigma_m) = 4\epsilon_m \left(\left(\frac{\sigma_m}{r_{ij}} \right)^{12} - \left(\frac{\sigma_m}{r_{ij}} \right)^6 \right), \quad (1)$$

where r_{ij} is the geometrical distance between two monomers i and j and ϵ_m and σ_m are set to 1, such that $V_{\text{LJ}}(r_{\text{min}} = 2^{1/6}) = -1$. As a remnant of the origin of the model [16] and in order to facilitate future enhancements and the comparison with previous studies, we introduce a weak bending stiffness, i.e., the polymer is not flexible in a strict way, but may be considered to be flexible in practice:

$$V_{\text{bend}}(\cos \theta_i) = \kappa (1 - \cos \theta_i), \quad (2)$$

where θ_i is the angle defined by the two bonds at monomer i and the bending stiffness parameter κ is here set to 1/4. The interaction between monomers and the string is also based on a simple Lennard-Jones potential, but we neglect, as usual [5, 13], the internal structure of the substrate, i.e., we assume a homogeneous “charge” distribution along the z -axis. We hence simply integrate to get

$$V_{\text{string}}(r_{z,i}; \epsilon_f, \sigma_f) = a \int_{-\infty}^{\infty} V_{\text{LJ}} \left(\sqrt{r_{z,i}^2 + z^2}; \epsilon_f, \sigma_f \right) dz = a \pi \epsilon_f \left(\frac{63 \sigma_f^{12}}{64 r_{z,i}^{11}} - \frac{3 \sigma_f^6}{2 r_{z,i}^5} \right), \quad (3)$$

where $r_{z,i}$ is the distance of the i th monomer perpendicular to the string and the potential is scaled by setting $a \approx 0.528$ for convenience [15, 17]. ϵ_f and σ_f are free parameters and can be considered as the string attraction strength and the effective “thickness” of the string, which is proportional to the equilibrium distance of the string potential, respectively. The overall energy of the system finally reads

$$E = \sum_{i=1, j>i+1}^{N-2} V_{\text{LJ}}(r_{ij}) + \sum_{i=2}^{N-1} V_{\text{bend}}(\cos \theta_i) + \sum_{i=1}^N V_{\text{string}}(r_{z,i}). \quad (4)$$

For estimating the ground-state energies, we apply generalized-ensemble Monte Carlo methods [18, 19]. Conformational changes are forced by applying a variety of update moves, including local crankshaft and slithering-snake moves and global spherical-cap and translation moves [17].

3. Results

We now discuss low-energy structures of the above described system for different values of the string-potential parameters σ_f and ϵ_f . Based on the simulation of more than hundred system parametrizations, we construct the full conformational phase-diagram which is shown in Fig. 1.

We identify four major conformational phases, which we denote Gi, B, C, and Ge. For small values of both σ_f and ϵ_f , i.e., for weak string attraction and small effective radius of the string, we find globular conformations with spherical symmetry surrounding the string (phase Gi). Increasing the string attraction strength, conformations stretch out along the string breaking the spherical symmetry and barrel-like conformations with the string inside emerge (phase B). In the case of very high string attraction we even find monolayer tubes with each monomer being in direct contact with the substrate. Due to the finite size of the system, these barrel-like structures break when increasing the effective diameter of the string and low-energy structures become clamshell-like (phase C), i.e., we find adsorbed conformations consisting of a few layers which are not wrapping the string completely. Finally, decreasing the string attraction at this effective radius, conformations become spherical droplets stuck to the string (phase Ge). Low-energy conformations from different regions are visualized exemplarily in Figs. 1 and 2.

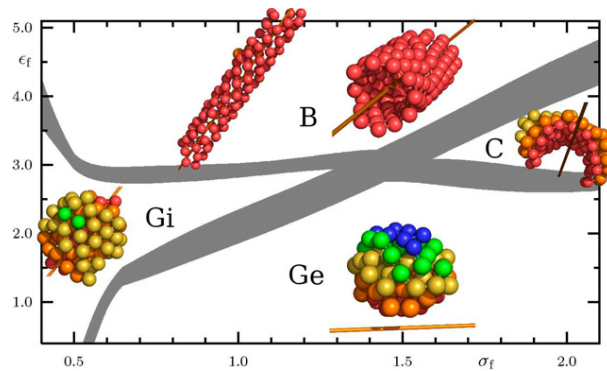


Figure 1: The low-energy conformational phase diagram for polymers adsorbed at nanostrings. From bottom to top, the string attraction strength ϵ_f increases, from left to right, the effective radius of the string σ_f becomes larger. Different monomer colors or shadings encode different distances from the string. Monomers near the equilibrium distance from the string (colored in red) are defined to be in contact with it.

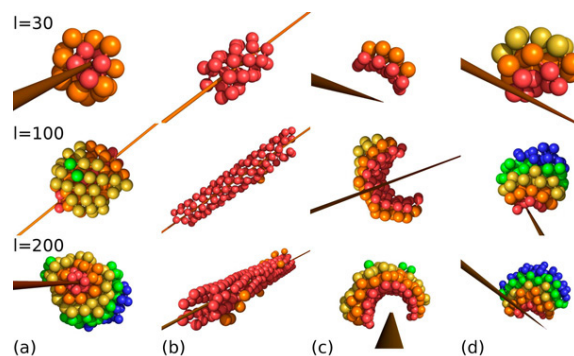


Figure 2: Visualizations of low-energy conformations with $N = 30, 100,$ and 200 monomers in phases (a) Gi, (b) B, (c) C, and (d) Ge.

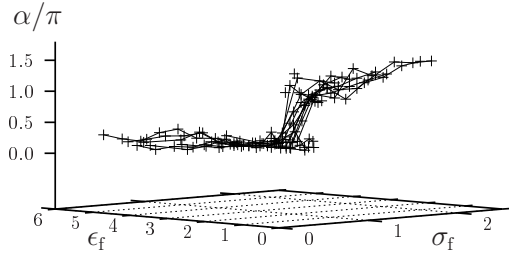


Figure 3: Opening angle, data points with same σ -value are connected by lines to guide the eyes. See also Fig. 2(a) and (b) for closed conformations ($\alpha/\pi \approx 0$) and 2(c) and (d) for open ones ($\alpha/\pi > 1$).

We convinced ourselves by simulating chains with lengths $N = 30$ and 200 that the general, qualitative structure of the conformational phase diagram does not depend on the actual length of the polymer, see Fig. 2 for examples. Of course, details like the exact positions of transitions lines may indeed depend on the actual polymer length.

To define the different phases and the crossover between them, we introduce observables showing a peculiar behavior at the transitions. In Gi and B, for example, the polymer conformations surrounds the string completely, in contrast to the structures in Ge and C. For the localization for the transition between $G_i \leftrightarrow G_e$ and $B \leftrightarrow C$, we hence look at the opening angle α [15] of the polymer conformation. The value of this angle shows a jump (low values for Gi and B, high values for C and Ge) at the crossover between these phases, which is shown in Fig 3. See [15] for more details on the localization of phase boundaries.

We finally would like to get at a deeper analysis of some structures in phase B. At very high attraction strengths, low-energy conformations become regular monolayer conformations wrapped around the string, i.e., single-walled tubes with an ordered arrangement of monomers form. It is noticeable, that there is a competition between different chiral angles, i.e., orientations of the wrapping. This behavior is of particular interest as it is in a similar manner known from carbon nanotubes [8]. Figure 4 illustrates the distribution of the chiral or wrapping angles of such a monolayer conformation. Therefore we unzip the structure, i.e., we project it onto a plane, and

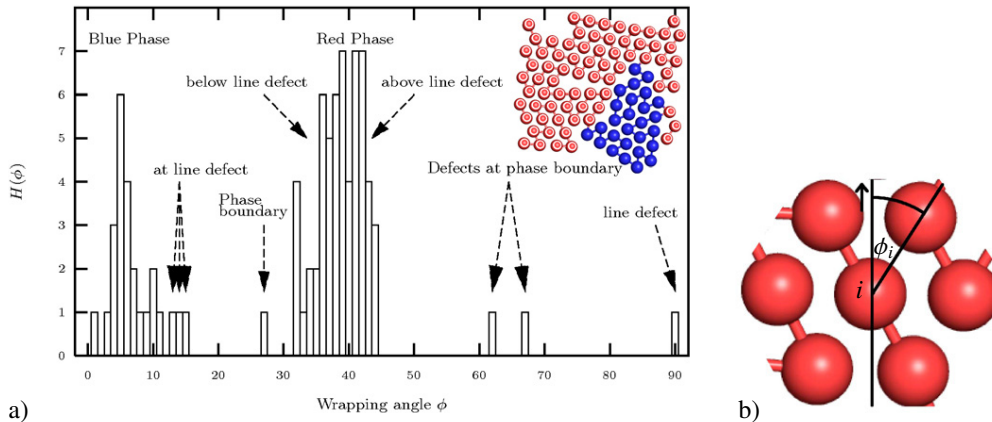


Figure 4: a) Angular distribution function of a monolayer structure with $\sigma_f = 1.569$ (also shown as inset picture in Fig. 1, phase B). Inset: Unzipped, planar representation. Different colors (red and blue, or light- and dark-gray, respectively) represent main regions with different wrapping angles. b) Illustration of the definition of the wrapping angle. The arrow points in the direction of the string.

measure the angular distribution function (adf) of this unzipped structure, whereas we define the chiral or wrapping angle ϕ_i of the i th monomer as the smallest angle between the vectors pointing to its neighbors and the vector in the string direction (see Fig. 4 b). In the adf we clearly see the signals from two different regions with different chiralities as well as from defects in that structure. A detailed, systematic analysis of monolayer structures at high string attraction strength and different effective string thicknesses is subject of ongoing studies [20].

Acknowledgment:. We would like to thank J. Adler and T. Mutat from the Technion Haifa for intense discussions. This work is supported by the Umbrella program under Grant No. SIM6 and by supercomputer time provided by the FZ Jülich under Project Nos. jiff39 and jiff43.

References

- [1] A. Milchev, K. Binder, Polymer melt droplets adsorbed on a solid wall: A Monte Carlo simulation, *J. Chem. Phys.* 114 (19) (2001) 8610.
- [2] M. Bachmann, W. Janke, Conformational transitions of nongrafted polymers near an absorbing substrate, *Phys. Rev. Lett.* 95 (2005) 058102.
- [3] M. Bachmann, W. Janke, Substrate specificity of peptide adsorption: A model study, *Phys. Rev. E* 73 (2006) 020901(R); Substrate adhesion of a nongrafted flexible polymer in a cavity, *ibid.*, 041802.
- [4] J. Luettmer-Strathmann, F. Rampf, W. Paul, K. Binder, Transitions of tethered polymer chains: A simulation study with the bond fluctuation lattice model, *J. Chem. Phys.* 128 (2008) 064903.
- [5] M. Möddel, M. Bachmann, W. Janke, Conformational mechanics of polymer adsorption transitions at attractive substrates, *J. Phys. Chem. B* 113 (11) (2009) 3314.
- [6] K. Goede, M. Grundmann, K. Holland-Nell, A. G. Beck-Sickinger, Cluster properties of peptides on (100) semiconductor surfaces, *Langmuir* 22 (2006) 8104.
- [7] M. Bachmann, K. Goede, A. G. Beck-Sickinger, M. Grundmann, A. Irbäck, W. Janke, Microscopic mechanism of specific peptide adhesion to semiconductor substrates, *Angew. Chem. Int. Ed.*, in press (2010).
- [8] M. S. Dresselhaus, G. Dresselhaus, P. Avouris (Eds.), *Carbon Nanotubes: Synthesis, Structure, Properties, and Applications*, Vol. 80 of Topics in Applied Physics, Springer, Heidelberg, 2001.
- [9] T. Hasan, Z. Sun, F. Wang, F. Bonaccorso, P. H. Tan, A. G. Rozhin, A. C. Ferrari, Nanotube-polymer composites for ultrafast photonics, *Adv. Mater.* 21 (2009) 3874.
- [10] M. Gao, L. Dai, G. G. Wallace, Biosensors based on aligned carbon nanotubes coated with inherently conducting polymers, *Electroanalysis* 15 (2003) 1089.
- [11] B. J. Carroll, Equilibrium conformations of liquid drops on thin cylinders under forces of capillarity. A theory for the roll-up process, *Langmuir* 2 (2) (1986) 248.
- [12] H. D. Wagner, Spreading of liquid droplets on cylindrical surfaces: Accurate determination of contact angle, *J. Appl. Phys.* 67 (3) (1990) 1352.
- [13] A. Milchev, K. Binder, Polymer nanodroplets adsorbed on nanocylinders: A Monte Carlo study, *J. Chem. Phys.* 117 (2002) 6852.
- [14] I. Gurevitch, S. Srebnik, Monte Carlo simulation of polymer wrapping of nanotubes, *Chem. Phys. Lett.* 444 (2007) 96; Conformational behavior of polymers adsorbed on nanotubes, *J. Chem. Phys.* 128 (2008) 144901.
- [15] T. Vogel, M. Bachmann, Conformational phase diagram for polymers adsorbed at ultrathin nanowires, *Phys. Rev. Lett.* 104 (2010) 198302.
- [16] F. H. Stillinger, T. Head-Gordon, C. L. Hirshfeld, Toy model for protein folding, *Phys. Rev. E* 48 (2) (1993) 1469.
- [17] T. Vogel, M. Bachmann, to be published (2010).
- [18] B. A. Berg, T. Neuhaus, Multicanonical ensemble: A new approach to simulate first-order phase transitions, *Phys. Rev. Lett.* 68 (1992) 9.
- [19] F. Wang, D. P. Landau, Efficient, multiple-range random walk algorithm to calculate the density of states, *Phys. Rev. Lett.* 86 (2001) 2050.
- [20] T. Vogel, T. Mutat, M. Bachmann, J. Adler, to be published (2010).